



EARTHQUAKE DATA AND MODELLING TO STUDY THE EFFECTS OF FUTURE EARTHQUAKES ON A FINAL REPOSITORY OF SPENT NUCLEAR FUEL IN SWEDEN

Göran BÄCKBLOM¹, Raymond MUNIER² and Harald HÖKMARK³

SUMMARY

Earthquakes have only on a few occasions exceeded magnitude 4 in Sweden in modern times. The safety case for a deep repository for spent fuel however includes an earthquake scenario as earthquakes with much greater magnitudes probably occurred in northern Sweden during the most recent deglaciation period some 9000 - 10 000 years ago when re-activated faults ruptured the surface over lengths of 150 km and such events may repeat in the future.

Underground field evidence of effects of earthquakes due to faulting have been collected from e.g. Italy, Japan, South Africa, Taiwan and the USA to support decision on how close to a displacing fracture zone a waste canister can be positioned. The field data are complemented with rock mechanics simulation of earthquakes using boundary element and explicit finite difference approaches. The extensive worldwide review of field data in combination shows that brittle deformation of a rock mass is predominantly located along reactivation of pre-existing fractures. The data emanating from faults intersecting tunnels show that creation of new fractures is confined to the immediate vicinity of the reactivated faults and that deformation in host rock is rapidly decreasing with the distance from the fault. By selection of appropriate respect distances the probability of canister damage due to faulting is further lowered. Comparison of field data and models indicate that "respect distances" between a fault and canister positions are considerably smaller than values predicted by numerical models.

INTRODUCTION

Swedish Nuclear Fuel and Waste Management Co. (SKB) www.skb.se, executes a comprehensive programme to implement a geological repository and start the deposition of spent nuclear fuel during the latter part of next decade, SKB [1]. It might appear surprising that there are concerns for earthquakes in one of the most tectonically stable areas in the world - the Baltic Shield. Only on a few occasions in modern times has earthquakes exceeded magnitude 4 in Sweden. Yet, analysis of the long-term safety of

¹ Conrox, www.conrox.com, goran.backblom@conrox.com

² Swedish Nuclear Fuel and Waste Management Co, www.skb.se, raymond.munier@skb.se

³ Clay Technology, www.claytech.se, hh@claytech.se

the deep repository includes an earthquake scenario because it has been demonstrated that earthquakes with much greater magnitudes most likely have occurred in northern Sweden during the most recent deglaciation period some 9000 - 10 000 years ago and that such events may repeat in the future. One of the most prominent evidences is the Pärvie post-glacial fault in Lapland, Sweden where the displacements exceeded 10 m in places and occurred over distances of around 150 km, Lundqvist [2]. The long term safety of the geological repository is ensured by isolation of the waste within the engineered and natural barrier system and SKB has studied the possible effects of faulting due to earthquakes, Bäckblom [3]. Of particular concern is that faulting may create new fracturing and reactivate previously existing fractures. In case fractures crossing the deposition hole for the long-lived spent fuel canisters slip more than an accumulated 0.1 m the canister may be damaged. Field observations of rock conditions close to re-activated faults and numerical modelling of rock mass response to faulting are complementary methods to estimate the proper "respect distance" from a fault that may reactivate in the future and the underground location where the spent fuel is deposited, see Figure 1.

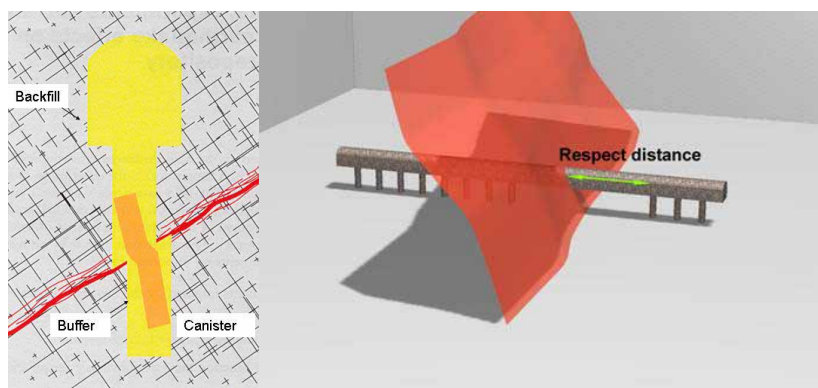


Figure 1. (Left) Accumulated fracture displacements > 0.1 m may impair the canister. (Right) By proper selection of "respect distance", possible damage by fault movements is mitigated

Local tunnel damages due to reactivation of cross-cutting faults have been compiled from cases in, Japan, South Africa, Taiwan and the USA. The rock mass response to faulting has been investigated by two conceptual approaches. The first static approach assumes that the re-activation of a fault cause displacements in a fractured rock mass, assuming zero friction along the fracture planes. The second approach includes friction along the fractures as well as the dynamic effects of the earthquakes. Assumptions and methodologies for the studies are explained as well as the main results.

METHODOLOGIES AND ASSUMPTIONS USED

Compilation of recorded earthquake damages

The study started with compilation of information by literature surveys, internet searches and by sending circular letters to around 60 organizations over the world asking for cooperation and possible information. Several previous compilations, for example Dowding [4], Power [5], Asakura [6] were re-visited. The data base used in Sharma [7] was also kindly provided by Prof. Judd and utilized. All these compilations and information provided by the contributors cover records from underground damages within a broad range of bedrock conditions, tunnel construction methods, depth to surface etc, Bäckblom [3]. It is evident that methods for seismological interpretation and classification of damages have changed over the years, from the oldest record in our study, the deformation of the Wrights tunnel in the San Francisco earthquake 1906, Prentice [8] to the latest, the faulting of a tunnel in Western Tottori, Japan in year 2000, Ueta [9]. The studies in general clearly evidence the scarcity of underground damages compared to the widespread

damages that occur at the surface at strong earthquakes. Of special interest in our study are the very few records on damages associated with reactivation of faults crossing tunnels or drifts. Based on the desk studies, site visits followed to South-Africa, Taiwan and Japan to discuss and review findings with the researchers having access to the basic information. The information from South Africa is direct and relevant, as the reactivated faults and sidewalls are readily available for observations from the unlined rock in the deep mines with, while the studies in Taiwan and Japan infer damages and deformations in the rock based on observations in the tunnel linings, road beds and railways.

Outline of modeling approaches

Fracture zones will obviously be avoided for deposition as the zones may reactivate in the future and displace more than 0.1 m thereby impairing the engineered barrier system. A remaining issue then is to estimate the possible extent of induced fracture shear displacements within the repository host rock that may result from a future earthquake of a given magnitude occurring at a given distance from a possible canister position. Four different modeling approaches, Table 1, have been used.

Table 1. Outline of four modeling approaches used

#	Conceptual idea with pro et con and code used
1	A slip is imposed at the primary fault. The static response of the linear elastic rock mass with inclusions of friction-less target fractures is calculated using the displacement-discontinuity method. The target fractures populations are generated utilizing site-specific lengths, strikes and dips +: A huge number of calculations possible with varying magnitudes, distances to target fractures and target fracture statistics -: Static effects are calculated but not the dynamic effects. Fractures must be friction-less. Code: POLY3D [10, 11]
2	A slip is imposed at the primary fault. The dynamic response of the linear elastic rock mass with inclusions of one target fracture with friction is calculated using a finite difference code FLAC3D for the target volume. The WAVE finite-difference code is used to simulate the dynamic boundary conditions for the FLAC3D calculations. WAVE provides a fair description of the processes at the rupture of the primary fault +: The dynamic effects of a distant earthquake are studied. The target fracture can have friction and other fracture properties like cohesion and stiffness. -: Static effects are not calculated. Only one target fracture. Only a few numbers of calculations are practically possible. Codes: WAVE [12] FLAC3D [13]
3	A slip is imposed at the primary fault. The combined static and dynamic response of the linear elastic rock mass with inclusion of one target fracture with friction is computed. +: Static as well as dynamic response -: Fractures must be aligned with the computational grid. Code: WAVE
4	The rock mass includes the primary fault and slip on that fault takes place as a result of potential instability +: Full static and dynamic response. -: Only one target fracture. Only a few computations are practically possible. Code: FLAC3D

The length of the primary fault has been selected based on empirical magnitude-length distributions, Wells [14]. We assume magnitude 6 events in the calculations. The imposed displacements at the primary fault are calculated from the relation $M_0 = G \cdot A \cdot d$ where M_0 is the seismic moment, determined by the rock shear modulus G , the rupture area A and the average fault slip d . The M_0 is calculated from $M = 2/3 \cdot \log M_0 - 6.07$, Scholz [15] where M is the moment magnitude. For dynamic modeling, approaches #2, #3 and #4, it is assumed that the rupture originates at the center of the rupture area and propagates outwardly with a speed that is a fraction (70%) of the shear wave velocity given by the rock elasticity parameters. Here Young's modulus is set at 75 GPa and Poisson's ratio at 0.25.

Transfer of results from case studies and modeling to the situation that may prevail at the state of rapid deglaciation in future

From the compilations reviewed in Bäckblom [3] it is evident that damages underground are very rare and basically not existing for Peak Ground Acceleration $<2\text{m/s}^2$. Such high accelerations are very unlikely in the Swedish bedrock within the next 50 years when the final repository is constructed and operated. Possible damages due to earthquakes are however studied for the situation at a future deglaciation, when stored elastic energy due to the ice load combined with tectonic energy from the Atlantic ridge-push are released and may cause post-glacial faulting in a manner similar to the 150 km long surface ruptured Pärvie-fault, Lundqvist [2]. In spite of the peculiar hydro-mechanical situation that may exist at the ice-front it is argued that data acquired from current earthquakes and their effects are relevant to assess possible creation of new fractures and the rock mass response due to earthquakes for a geological repository. However most data from underground damage emanates from plate boundaries where strike-slip fault displacements dominate. Significant strike-slip components can be demonstrated at post-glacial faults, but the reverse faulting component appears to dominate. In spite of this we find it reasonable to believe that the effects of “glaciation-induced” earthquakes, once triggered should not significantly differ from the “mining-induced” or “natural” earthquakes and therefore, many general and empirical relations should apply.

UNDERGROUND DAMAGE DUE TO FAULTING

Most damages recorded underground are due to shaking, but a few cases are reported where faults that cross underground openings have reactivated, Table 2. Where direct exposure of the rock is possible, like in the underground mines in South Africa, it is evident that damage in the rock is within the complex fault zone or in its close vicinity. The damages in tunnel linings are also recorded within a few meters of the fault, see for example Figure 2 (left) substantiating the same conclusion. However, deformations of tunnel linings and installations may extend for some hundred meters from the fault, see for example Figure 2 (right). The Inatori measurements as most of the other measured observations (Table 2) are not direct observations on the rock, but on the tunnel lining or along rails and it is conceived that the deformations in the rock is much less than measured dynamic effects inside the tunnels.

The studies on underground damages due to earthquakes further corroborates that displacements in the rock due to earthquakes predominantly is by reactivation of pre-existing faults (that are avoided in the repository design) and that possible new fracturing in the rock would be delimited to the vicinity of the reactivated faults which also is in line with a comprehensive study along a post-glacial fault in Sweden, Bäckblom [16].

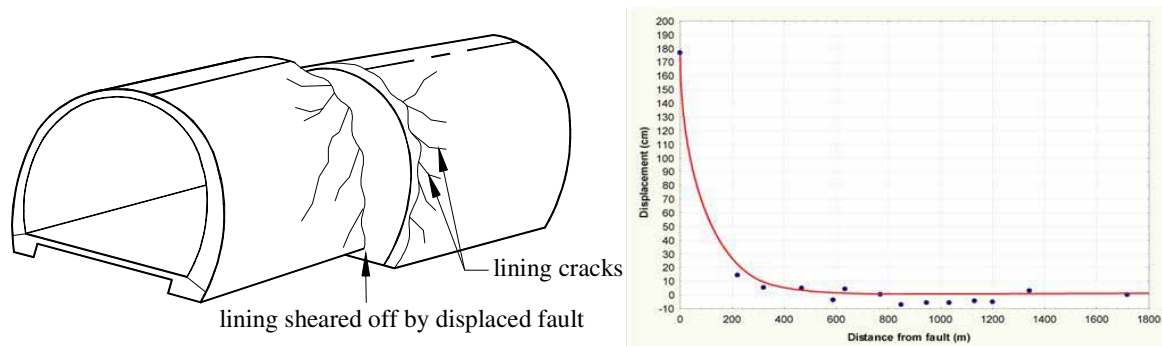


Figure 2. (Left). Example on damage. Concrete lining at the Shih-Gang Dam tunnel, Chi-Chi, 1999, Taiwan Wang [17] (Right). Deformations along the Wrights tunnel, San Francisco, 1906, USA. Based on Prentice [8].

Table 2. Cases of reactivated faults crossing underground openings, SKB [3].

Tunnel Selection of reference	Date, Magnitude, Depth Length of reactivated fault crossing the tunnel/drift. Distance to epicentre, R Fault displacement	Deformations, Observations
Tanna, Japan Kawaguchi [18]	Nov 26, 1930, M =7.1, D =11km 24km surface rupture, R= 15km, Left-laterally 2.7m, 0.6m vertically	A few cracks in the main tunnel in spite of being around 0.5m from the active shear zone. Collapse of a drainage tunnel.
Inatori, Japan Kawakami [19]	Jan 14, 1978, M =7, D =3km 18km main fault and a 3km subsidiary surface fault cut by the tunnel. R= 23km. Right-lateral 0.7m	0.5 – 0.7m displacement within a zone of 20 m. Deformations as measured on the lining, show kinks in the order of decimetres 300 – 400 metres from the fault when measured on the concrete lining.
Shioya-Danigawa, Japan Asakura [6]	Jan 17, 1995, M=7.2, D= 18km 5km fault, R= 8km. Right-lateral 1cm, vertical 5cm as measured between upstream and downstream tunnel.	8-cm lateral and 5-cm vertical relative displacement of the lining and with cracks confined within a 10m long zone around the fault crossing.
Tottori, Japan Ueta [9]	Oct 6, 2000, M= 7.3, D= 10km 2km disguised active fault. R= 8km.	Damage in concrete lining is limited to a few metres from the fault The headrace tunnel was left-laterally displaced 10-20cm.
Mathjabeng mine, South Africa Dor [19]	Apr 22, 1999, M = 5.1, D= 2km 50km. R= 1 km.Normal dip-slip 40cm	Co-seismic displacement and massive increase in surface area is distributed over many gouge zones over a 30m wide zone.
A.R.M, Shaft # 5, South Africa Bäckblom [3]	Aug 1, 2001, M= 4.2, D= 2km 5 km long fault, R < 1km. 20cm slip	Damage to the rock (except rock fall and tunnel closures) within some 10m from the fault (study in progress).
Shih-Gang Dam Tunnel, Taiwan Wang [17]	Sept 21, 1999, M=7.3, D =8 km 96 km of surface rupture, R = 47km. 4m vertical and 3m horizontal displacement.	Damages to the concrete lining is confined to within a few metres from the fault
BART-tunnels, USA Brown [21]	Several displacement due to slips along the Hayward fault, > 80km long	70 % of measured deformation from reference line within 50m of the fault. Fault creep restricted to a zone < 250m from the fault.
Wrights tunnel, USA Prentice [8]	Apr 18, 1906, M= 7.8, D =20km San Andreas Fault, Rupture length 470km, R= 70km Strike-slip 1.7 - 1.8m	60-85% of the co-seismic slip at the San Francisco 1906 earthquake occurred along a single fault plane. The remainder of the offset is distributed within a few hundred meters of the principal fault plane.

MODELLING OF ROCK MASS RESPONSE DUE TO FAULTING

Concepts

Figure 3 (right) illustrates the conceptual representation of the problem addressed in the studies. The earthquake is represented as a slip event taking place along a single planar fault - “the primary fault”. The dynamic and quasi quasi-static stress changes induce shear movements along fractures, “target fractures”,

located at varying distances from the epicenter and from the edges of the rupture area. The amount of induced displacements at the target fractures depends on a number of factors: the distance from the hypocenter to the target fractures, the type of stress disturbances produced by the slipping primary fault, the relative orientation of the primary fault and the target fractures, the size of the target fractures, the mechanical properties of the host rock in general and of the target fractures in particular, etc. The slipping primary fault will generate both dynamic effects and permanent static effects. It is worthwhile to note that the moment magnitude is a measure of the total energy released through the earthquake. It does not necessarily have to determine the nature of the impact on the rock stresses. A modest average slip on very large rupture area may release the same energy as a large average slip on a small rupture area, but will not have the same impact on the surrounding nearby rock. The stress drop $\Delta\sigma$, i.e. the change in primary fault shear stress, is likely to be more decisive of the effects on nearby rock and target fractures, as least as far as permanent, static effects are concerned. It is anticipated that faulting may occur during future glaciation-deglaciation cycles, Figure 3 (left). Examples of results from the four modeling approaches are described in the following.

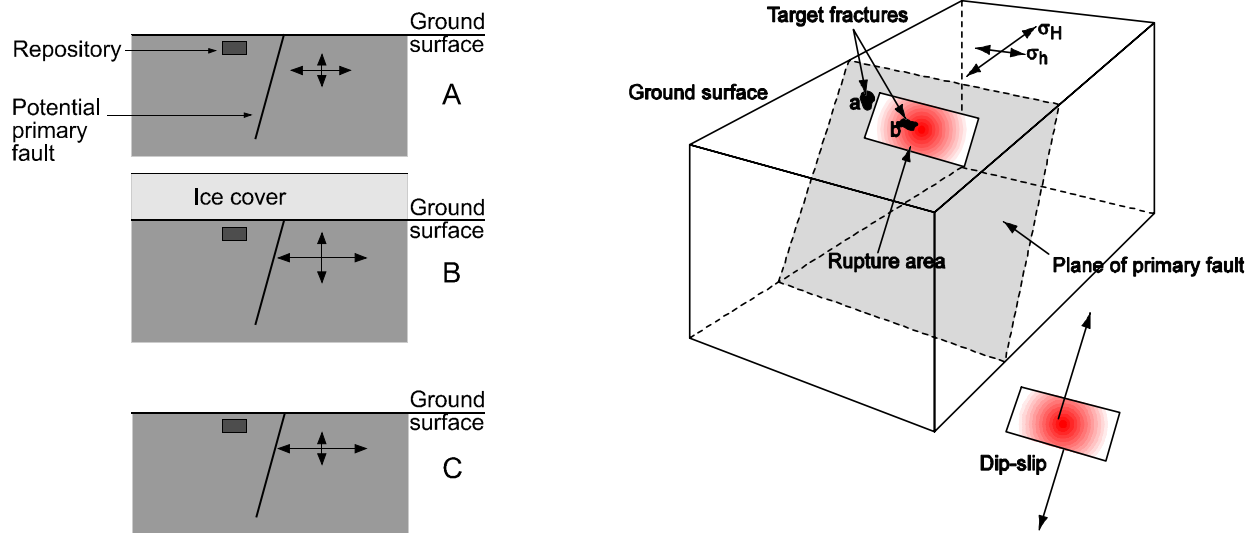


Figure 3. Conceptual models in a geological context assuming future glaciations and deglaciations. Left: present-day rock stresses (A), stresses under a future ice cover (B) and post-glacial stresses (C) after the ice retreat. Right: Conceptual model of primary fault and the target fractures, Hökmark [22]. The rupture originates at the center of the rupture area and propagates outwardly with a speed that is a fraction (70%) of the shear wave velocity given by the rock elasticity parameters.

Approach #1. Static analyses using POLY3D

The numerical formulation allows for simulation of many thousand stochastically generated earthquakes that induce displacements on site-specific statistical populations of repository host rock fractures, La Pointe [10]. The individual fractures do not interact, meaning that one POLY3D run is equivalent to as many single-fracture analyses as there are fractures in the statistical sample. Figure 4 shows an example. An earthquake of moment magnitude 6.1 is assumed at a distance of 2 km from the edge of a rock volume containing a population of hexagonal shape fractures with radii between 0 and 120 m. The calculated maximum displacements range between 0 mm and about 2.1 mm. The largest fracture in the statistical sample has a diameter of 240 m and moved less than the 80 m diameter fracture giving the largest displacement. This suggests that the maximum displacement in the sample might have been significantly larger if the 240 m fracture had been located and oriented as the 80 m fracture.

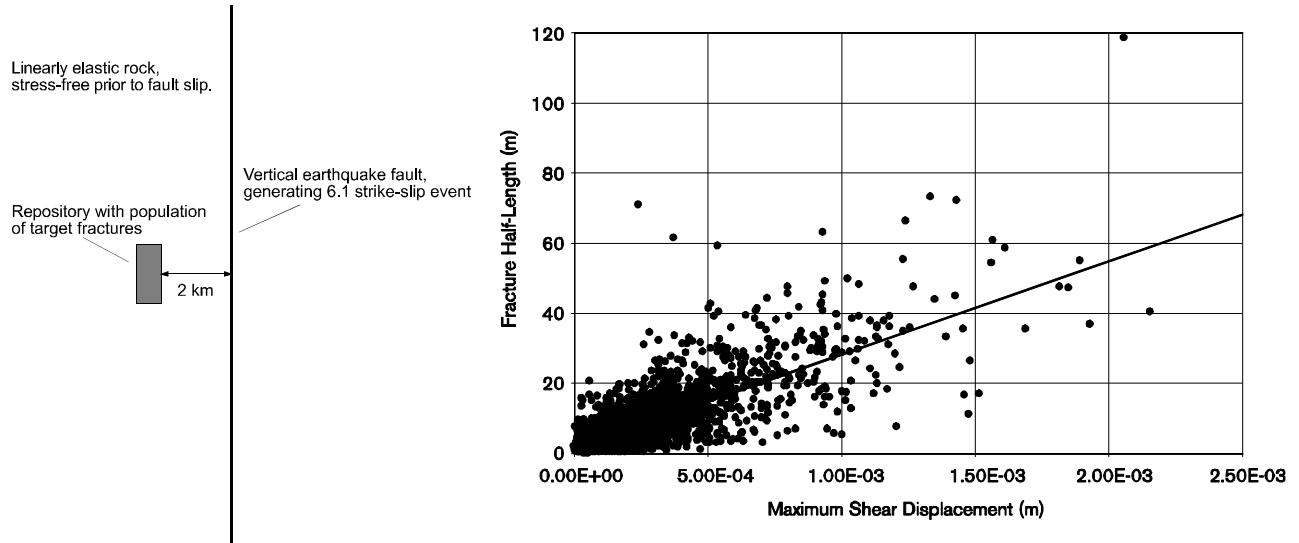


Figure 4. Example of simulations made with POLY3D. The primary fault is forced to slip by a prescribed amount. The effects of that slip on the initially stress-free rock volume containing a statistical population of target fractures are calculated. The orientation and the exact location of the individual fractures are not accounted for here.

Approach #2. Dynamic analyses using WAVE/FLAC3D

A number of dynamic finite difference calculations using the code FLAC3D have been conducted for which the seismic input was generated by use of the finite difference code WAVE, Hökmark [22]. A dip-slip event of magnitude 6 was simulated with WAVE, and the velocity records at a number of distances from the slipping fault were translated into stress-time histories. These were applied as plane wave dynamic boundary conditions at the base of the FLAC3D model. Figure 5 shows the interrelation between the WAVE model and the FLAC3D model, while Figure 6 shows sequences of snapshots from the WAVE model, i.e. the rupture development at the primary fault. The construction of the WAVE/FLAC3D modeling approach implies that only the oscillating effects of the seismic event are transferred to the target fracture, while the static or permanent effects are disregarded.

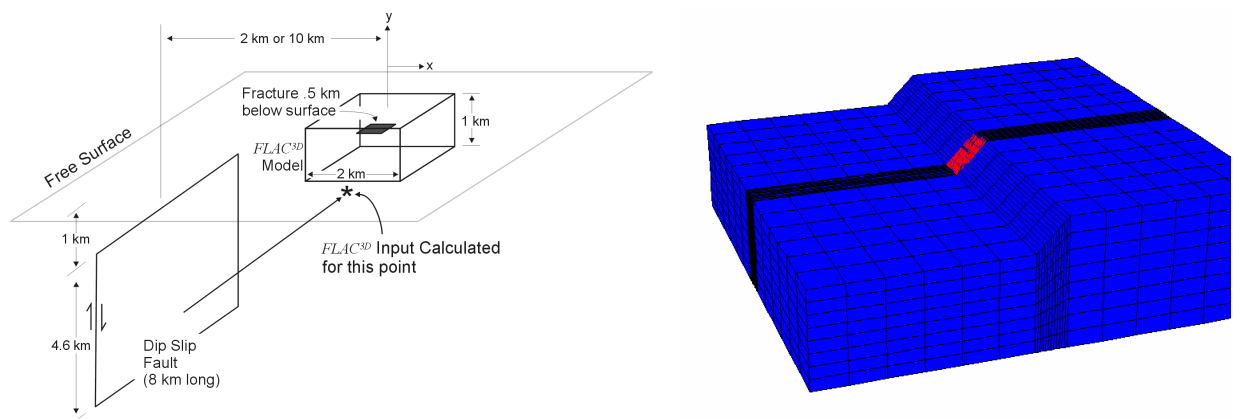


Figure 5. Modeling technique used in WAVE/FLAC3D study. Left: Velocity records from WAVE simulation of a magnitude 6 dip-slip event were translated into plane wave dynamic boundary conditions for a separate FLAC3D model. Right: FLAC3D model with upper part removed to display the interior. The 200m · 200 m target fracture is in red. The boundary condition was applied at the base of the model. All boundaries except the ground surface top boundary were viscous to eliminate effects of irrelevant wave reflections.

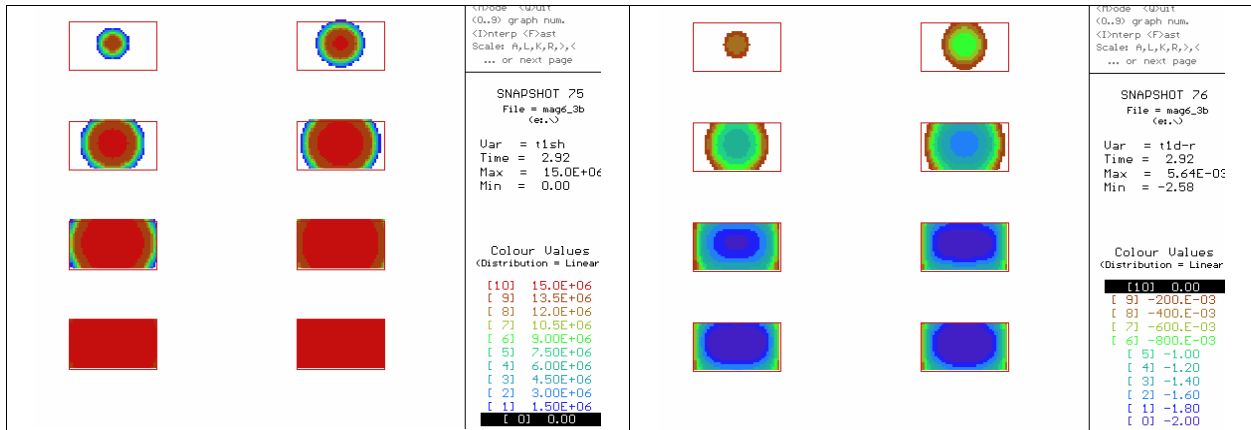


Figure 6. WAVE representation of rupture time-history sequence for dip-slip event with stress drop $\Delta\sigma=15$ MPa. The rectangles represent the 8.0 km by 4.6 km rupture area. Left hand plot shows shear stress (Pa) along the direction of slip. Right hand plot shows the slip displacement (m). For each plot, eight time-lapse images are shown, giving a longitudinal view of the fault at 0.75, 1.06, 1.37, 1.68, 1.99, 2.31, 2.62 and 2.93 seconds after the rupture initiation.

Approach #3. Combined static and dynamic analyses using WAVE

The WAVE code may be used to generate velocity records and stress records as an input to other models such as described above, but also to calculate the effects on target fractures so the static and dynamic effects are captured simultaneously. The limitation however is that fractures cannot have arbitrary orientations, but need to be aligned with the coordinate axes of the orthogonal finite difference grid. Figure 7 (left), shows results obtained using the WAVE code, Hökmark [22]. A dip-slip magnitude 6 event induced displacement on a 200 m diameter frictionless horizontal fracture at distances ranging between 200 m and 7000 m from the epicenter. The static, residual effects clearly dominate, in particular for the shortest distances. The right part of Figure 7 shows the result for the 2000 m distance case, now compared with corresponding WAVE/FLAC3D result. Both results are based on the same source, i.e. the rupture generated with WAVE as shown in Figure 6. The right part illustrates in a lucid way how the residual effects are captured in the WAVE model, but filtered off in the WAVE/FLAC3D modeling approach.

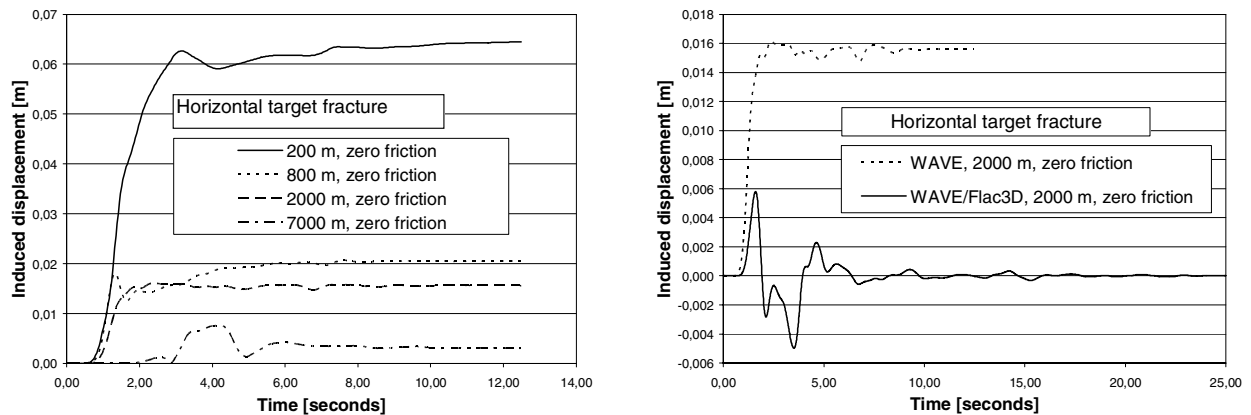


Figure 7. Calculated fracture displacements for a magnitude 6 earthquake. Left: Induced displacements on a 200 m diameter fracture at varying epicenter distances (200 m to 7 000m), computed with the WAVE code. Right: Comparison between WAVE result and corresponding WAVE/FLAC3D result.

Approach #4. No imposed slip on the primary fault. Full static and dynamic analyses using FLAC3D

In the analyses described above the slip was imposed on the primary fault without any coupling to the stress field or to the mechanical properties of the fault. This means that the slip was not modeled as a result of potential fault instability. Figure 8 shows a FLAC3D model containing the primary fault as well as the target fracture, Hökmark [22]. Here, an initial stress field was defined as indicated in Figure 3. The fault was given friction properties that made it potentially unstable and cohesive bonds to prevent it from slipping. The slip was simulated by releasing the bonds in a sequence that reproduced the rupture propagation shown in Figure 6. Examples of results are found in Figure 9. The left graph show results from corresponding WAVE analysis for comparison. The induced target fracture displacement is about half of the displacements found in the WAVE model. Part of the reason is the difference in epicenter distance. The right graph illustrates effects of target fracture friction. For the case analyzed here, a modest friction angle inhibited most of the induced movement.

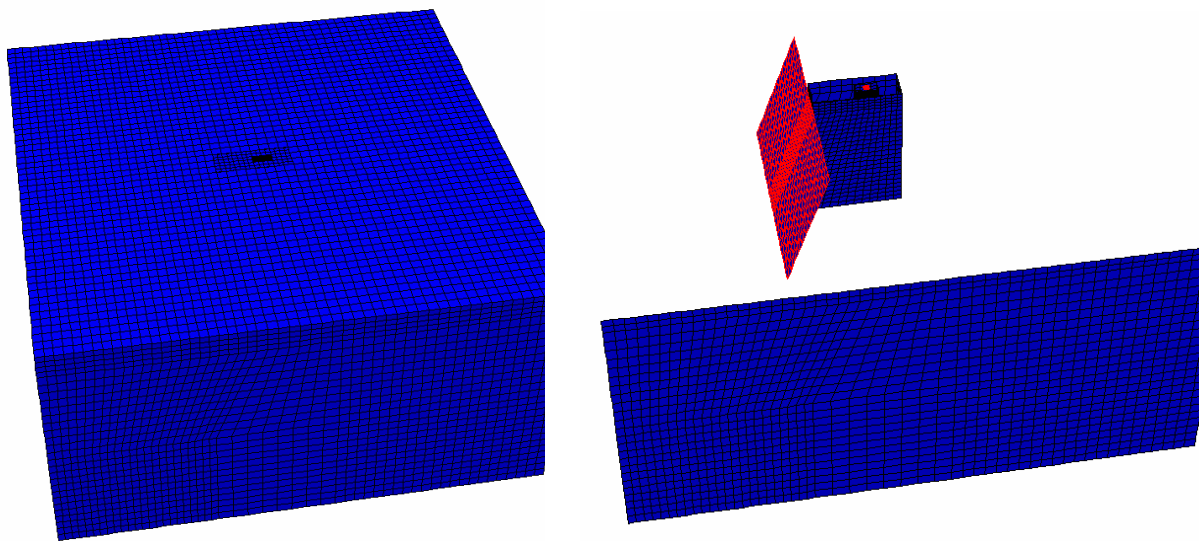


Figure 8. Left: The entire model volume of the FLAC3D model (20000m · 20400 m · 10000 m). Right: Same as left, but only selected parts visible to display the 8.0 km by 4.6 km rupture area and the horizontal target fracture. The horizontal fault-target distance is 2000 m, while the epicenter distance is about 3000m.

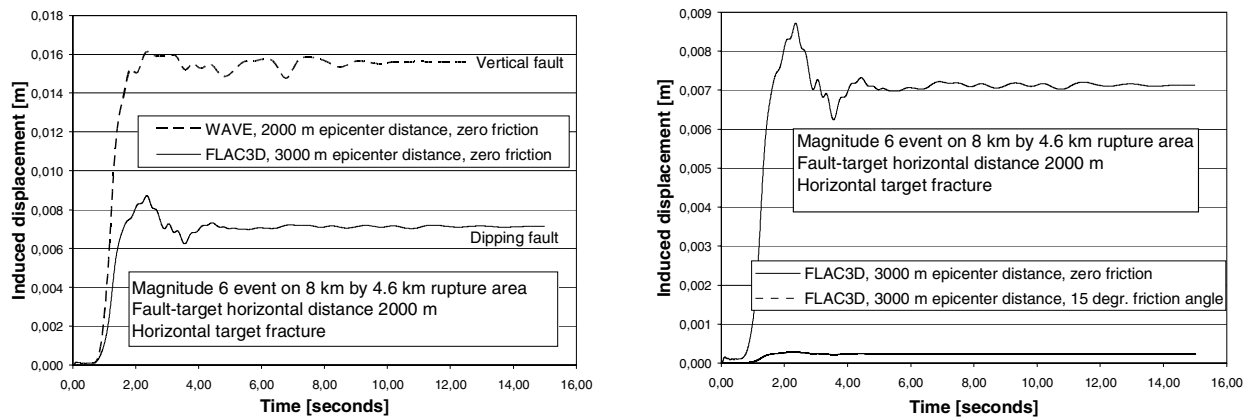


Figure 9. Shear displacement on target fracture, calculated with account of initial stress and primary fault properties. Left: comparison with WAVE result. Right: influence of target fracture friction.

Modeling results discussion and summary

All dynamic analyses have regarded earthquakes of moment magnitude 6 and these calculations show that displacements at target fractures are less than 0.1 m for target fracture diameters less than 200 m and for source-target distances of 200 m and larger. Numerically it would be very demanding to analyze much larger events in a similar way as has been demonstrated for magnitude 6. A magnitude 8 earthquake, for instance, releases about a thousand times more strain energy than a magnitude 6 earthquake, and would require a much larger rupture area. This means that the model size must be correspondingly larger, while the refinement of the calculation grid must be kept at the minimum size-independent level required to propagate the shear and pressure waves properly. Moreover, there is no clear-cut answer to the question of how to represent very large earthquakes in a physically relevant way. The seismic moment depends on the size of the rupture area and is a measure of the amount of released strain energy, but it does not necessarily have to determine the nature of the stresses acting on nearby target fractures. The stress drop, which is a function of the initial stresses and the residual fault strength, is likely to be the determining quantity, rather than the seismic moment. There are theories proposing that the stress drop is magnitude-independent, Scholz [15], and that a typical intraplate event should have a stress drop of around 15 MPa, i.e. the value assumed in the dynamic numerical studies described above. Therefore the results found for magnitude 6 earthquakes may be relevant also for larger events. This means that the 0.065 m induced displacement calculated for the 200 m distance between the reactivating primary fault and a 200 m diameter target fracture may indicate that 200 m would be a respect distance, given that 200 m diameter fractures and larger are avoided at actual canister positions. In case it would be possible to detect and avoid even smaller fractures, the computed respect distance would also be smaller. However, some more work will be needed to examine the importance of magnitude and stress drop. Results of very preliminary calculations suggest that extending the rupture area laterally in a numerical model of the approach #4 type will not lead to larger induced displacements on nearby target fractures, and that much larger stress drops can be obtained only if unrealistic initial stress fields that would cause extensive failure in the surrounding rock mass are assumed.

The different modeling approaches seem to give reasonably consistent results, such that differences are either small or can be explained by differences in the level of modeling detail. This improves the general confidence in the work conducted so far. However, there are still issues that need further attention. The importance of the orientation of the target fractures, for instance, needs to be examined systematically.

Induced displacements calculated by use of the POLY3D code include only the static component, i.e. the results would not be different if the slip on the primary fault would take place by a slow aseismic process, rather than by a sudden rupture. However, this particular limitation does not seem to be of decisive importance, since the WAVE and FLAC3D results (approaches #3 and #4) indicate that the static component dominates for short source-target distances. The maximum displacement, 2.1 mm, found in the POLY3D analysis for the 2 km distance (Figure 4, right) is much smaller than the 16 mm displacement found in the WAVE model for that distance (Figure 7, right). This is an apparent misfit, caused by the size distribution in the statistical sample and not a result of ignoring the dynamic effects: if all fractures had a 200 m diameter as assumed in the other approaches, the maximum induced displacement would be much larger, Hökmark [22]. Yet, this does not mean that it always will be sufficient to conduct purely static analyses. The importance of friction, for instance, may be different in dynamic and static models.

The WAVE/FLAC3D technique is relevant for analyzing effects at large distances where oscillations are the main concern and in cases where even modest oscillations may cause serious damage. For the deep repository, however, small distances between earthquake faults and target fractures are of paramount importance to analyze. As a consequence, permanent static effects will be the main concern, meaning that the WAVE/FLAC3D approach will not be a main tool in the continued work. Oscillating loads on target fractures and in the near-field may however be important for issues that concern, for instance, possible

changes in the mechanical properties of the bentonite buffer, so the WAVE/FLAC3D approach will continue to be a relevant option for some purposes.

The WAVE results are conclusive and include static as well as dynamic components of the effects on target fractures. The limitations concern the geometry, i.e. the orientation of fault and target fracture, and the way fault slip takes place, i.e. as a prescribed movement rather than as a movement powered by the stress field.

The FLAC3D approach is obviously the most developed and realistic one, and captures all aspects of the source target- interaction the way it is described conceptually in Figure 3 (right). At present, the approach has been applied only to a very small number of cases, and mainly for comparison with results obtained with the more simplistic approaches. In the continued work, FLAC3D models with smaller source target-distances and with other target fracture orientations will be analyzed.

All modeling approaches are based on the assumption of a linearly elastic host rock. This assumption implies that no energy is expended on fracturing or friction work. The conservativeness inherent in this assumption needs to be exploited further in coming work. The preliminary attempts made so far indicate that induced displacements in general should be expected to be significantly reduced if, for instance, fracturing around the tips of target fractures is accounted for, La Pointe [23]. Also the choice of earthquake parameters made here, i.e. with a high stress drop and a small rupture area, is conservative. According to regression relations found in the literature, Wells [14] a typical magnitude 6 dip-slip event should have a rupture area of about 100 km², while the rupture area was set at 37 km² in the dynamic analyses described here.

The idealized representation of fault movements used in the numerical models sets bounds to the range of source-target distances that can be considered, irrespective of the conservativeness of the input assumptions. Earthquake faults are represented by planar features in all models and seismic events are modeled as idealized and schematic relative movements along these planes. Attempting to analyze effects on target fractures at very small distances is not meaningful, since details in the fault geometry and in the source mechanism will become important in the vicinity of the fault. At small distances it is, for instance, not relevant to distinguish between induced displacements on target fractures and displacements on components of the seismogenic fault itself. Distances that are smaller than the measure used to describe the zone half-width should probably be considered too small in that respect.

MISCELLANEOUS STUDIES

This paper addresses whether future earthquakes may cause accumulated displacement > 0.1 m over the canister with the conclusion that such an event is not likely when the fracture length crossing the deposition holes are short (radii < 100m). The response of the bentonite and the canister to rapid fracture shear movements has been examined in laboratory tests and in numerical finite element analyses, Börgesson [24]. The objectives of these studies were to find out how the fracture shear velocity, the buffer density and the location and orientation of the shear plane in relation to the canister will influence the way forces are transferred from the moving rock to the canister, and how these conditions impact the scope and extent of canister deformations. The results will be used to examine the relevance and validity of the 0.1 m threshold displacement used as canister failure criterion in the safety assessment work. Although some work will be required, preliminary interpretations of the results suggest that the 0.1 m threshold is well on the conservative side.

Other issues that warrant studies are the possible hydro-mechanical effects due to earthquakes such as liquefaction that would cause the canister to sink through the surrounding buffer and in such way impair the barrier performance. However, by using a highly compacted saturated bentonite with densities around

2000 kg/m³ the risks for liquefaction are eliminated assuming earthquakes up to magnitude 7-8, Pusch [25]. The static load on the canister is assumed to be the swelling pressure of the buffer plus the water pressure added on the outside of canister. Earthquakes cause changes to groundwater levels, Muir-Wood [26] also these temporary changes are to be accounted for in the canister design. We were however unable to find field data supporting friction-loss in subsidiary faults and fractures due to the transient water-level changes that suddenly would reduce normal stresses acting on faults and fractures. As described in the previous section, the POLY3D model is very conservative in assuming that all fractures in the fracture network possess no friction whatsoever.

DISCUSSION

Earthquake damages underground are very limited compared to the corresponding damages at the ground surface as underground structures are strongly coupled to the rock with low potential for attaining the resonance frequency and surface waves being nearly absent at the high-velocity layer where underground openings are located compared to the low-velocity layer where the buildings are located. From the compilations made, underground damage due to shaking are recorded at peak ground acceleration at about 2 m/s² or higher. Such high accelerations are unlikely in the Swedish bedrock for the time period when the repository will be open, Wahlström [27]. However strong earthquakes may occur at future deglaciations, but the field data and numerical modeling imply that the effects mainly take place in the fault in itself with limited impacts outside the fault. While there are theoretical and physical limitations on maximum displacement at a fracture with given length, trace length distributions are key data for assessing the potential accumulated displacement over a deposition hole at a given earthquake. The numerical studies indicate that deposition holes crossing fractures with radii < 100 m would slip less than the 0.1 m threshold when subjected to the effects of a fault displacement corresponding to a 15 MPa stress drop magnitude 6 event at a distance of 200 m. The field data suggest that effects like new fracturing would occur only within a few meters from the boundary of the fault. "Respect distances" should then initially be wide enough to accommodate the fault and its "transition zone" or "process zone" that may be around 1 % of the fault length, Vermilye [28]. Site and fault specific studies in the process zone may considerably diminish the extent of the respect distance. Examples are if no field evidences for young reactivations are found in the nominal process zone or trace length distribution of fractures show that positions with long fractures may be excluded when the deposition hole are constructed. The studies would imply that the respect distance from a fault that may reactivate in the future and the closest location of deposition holes rather are tens of meters than hundreds of meters.

CONCLUDING REMARKS

Geological disposal is the preferred method for disposal of high-level and long-lived waste. From seismic point of view underground disposal is much preferred to any surface storage. The studies here corroborate previous knowledge that major displacements take place at reactivating faults and that new fractures may be created during this reactivation, but only in the close vicinity of the reactivated faults. In the proper design of the geological repository major and minor fracture zones that may be earthquake faults are of course avoided for deposition. A nearby fault reactivation may trigger fracture slips in the repository host rock but the conservative model approaches used shows that target fracture displacements are small (less than 0.1 m) for fracture radii < 100 m. By sampling the fracture lengths in the field and avoiding canister positions intersected by long fractures, the probability of impaired barrier functions due to earthquakes would be minimal.

ACKNOWLEDGEMENTS

The authors acknowledge the colleagues from 30+ organizations in Israel, Italy, Japan, South Africa, Sweden, Taiwan and USA that contributed to the results. Thanks are extended to Mark Christianson, Itasca Inc. Minnesota, and to Calum Baker, Applied Seismology Consultants Ltd, Shrewsbury, U.K., who performed the dynamic analyses. The financial support from Svensk Kärnbränslehantering AB (SKB) Sweden is acknowledged.

REFERENCES

1. SKB, "RD&D Programme 2001". Svensk Kärnbränslehantering AB, Stockholm, 2001. (SKB reports are in general downloadable from www.skb.se)
2. Lundqvist, J. and R. Lagerbäck . "The Pärve Fault: A late-glacial fault in the Precambrian of Swedish Lapland." GFF 98(1): 45-51, 1976
3. Bäckblom, G. and Munier, R." Effects of earthquakes on the deep repository for spent fuel in Sweden based on case studies and preliminary model results." SKB Technical Report TR-02-24. Svensk Kärnbränslehantering AB, (SKB). Stockholm, 2002
4. Dowding, C. H. and Rozen, A., "Damage to rock tunnels from earthquake shaking." American Society of Civil Engineers, Journal of the Geotechnical Engineering Division 104(2 Feb): 175-191, 1976
5. Power, M. S., Rosidi D. and Kaneshiro, J., Y. "Seismic Vulnerability of Tunnels and Underground Structures Revisited,, Newport Beach, CA,, Balkema, Rotterdam, The Netherlands, 243-250, 1998.
6. Asakura, T. and Sato Y., "Mountain Tunnels Damage in the 1995 HYOYOKEN-NANBU Earthquake". Railway Technical Research Institute (RTRI), Japan. 39(1), 9-16, 1998.
7. Sharma, S. and Judd, W.R. "Underground opening damage from earthquakes." Engineering Geology, 30 (3-4). 263-276, 1991.
8. Prentice, C. S. and Ponti, D.J. (1997). "Coseismic deformation of the Wrights Tunnel during the 1906 San Francisco earthquake; a key to understanding 1906 fault slip and 1989 surface ruptures in the South Santa Cruz Mountains, California." Journal of Geophysical Research, B, Solid Earth and Planets, 102(B1): 635-648, 1997.
9. Ueta, K., Miyakoshi, K. and Inoue, D. "Left-lateral deformation of head-race tunnel associated with the 2000 Western Tottori earthquake", Journal of the Seismological Society of Japan, 54(2), 547-556, (in Japanese), 2001.
10. La Pointe, P., Wallman, P., Thomas, W. and Follin, S. "A methodology to estimate earthquake effects on fractures intersecting canister holes" TR-97-07. Svensk Kärnbränslehantering AB, (SKB). Stockholm. 1997.
11. Thomas, A.L. "POLY3D: A three-dimensional polygonal element displacement discontinuity boundary element computer program with application to fractures, faults and cavities in the earth's crust" M.S. thesis. Stanford University, California. 1993.
12. Hildyard, M.W., Daenkhe, A. and Cundall, P.A. "WAVE: A computer program for investigating elastodynamic issues in mining." Proc. of 35th U.S. Symposium on Rock Mechanics, 519-524. 1995.
13. Itasca Consulting Group, Inc. "FLAC3D (Fast Lagrangian Analysis of Continua in 3 dimensions)". Version 2.0. Minneapolis. 1997.
14. Wells, D.L. and Coppersmith, K.J. "New empirical relationships among magnitude, rupture length, rupture width, rupture area and surface displacement." Bulletin of Seismological Society of America, 84(4), 974-1002, 1994.
15. Scholz, C.H. "The mechanics of earthquakes and faulting" Cambridge University Press. 1990.

16. Bäckblom, G. and Stanfors, R. "Interdisciplinary study of post-glacial faulting in the Lansjärv area Northern Sweden 1986 – 1988". TR 89-31 Svensk Kärnbränslehantering AB (SKB). Stockholm. 1989
17. Wang, W.L., Wang, T.T., Su, J.J., Lin, C.H., Seng, C.R. and Huang, T.H. "Assessment of damages in mountain tunnels due to the Taiwan Chi-Chi earthquake. Tunnels & Underground Space, 16 (3). 133-150. Pergamon Press. 2001.
18. Kawaguchi, A., "Special report of the Kita-Izu earthquake. An illustrated construction review. Koji Gaho, 7(2), 2-31, 1931. (In Japanese).
19. Kawakami, H., "Evaluation of deformation of tunnel structure due to Izu-Oshima-Kinkai earthquake of 1978. Earthquake Engineering & Structural Dynamics", 12(3): 369-383. 1984
20. Dor, O., Reches Z., and van Aswagan, G."Fault zones associated with the Matjhabeng earthquake, 1999, South Africa." Rockburst and Seismicity in Mines, RaSiM5 (Proceedings), South African Inst. of Mining and Metallurgy, 109-112. 2001
21. Brown, I. R., Brekke, T.L. and Korbin, G.E. "Behavior of the Bay Area Rapid Transit tunnels through the Hayward Fault." Report No. UMTA-CA-06-0120-81-1. Washington D.C.U.S. Department of Transportation, Urban Mass Transportation Administration. 1981.
22. Hökmark, H., Christianson, M., Baker, C. and Munier R. "Respect distances –Rationale and means of computation" Svensk Kärnbränslehantering AB (SKB). Stockholm. 2004. In preparation.
23. La Pointe, P., Cladouhos, T., Outters, N. and Follin, S. "Evaluation of the conservativeness of the methodology for estimating earthquake-induced movements of fractures intersecting canisters". TR-00-08. Svensk Kärnbränslehantering AB, (SKB), Stockholm, 2000.
24. Börgesson, L. and Johannesson, L-E. "Earthquake induced rock shear through a deposition hole. Effect on the canister and the buffer." TR-04-02. Svensk Kärnbränslehantering AB, (SKB). Stockholm, 2004.
25. Pusch, R. "On the risk of liquefaction of buffer and backfill" TR-00-18. Svensk Kärnbränslehantering AB, (SKB). Stockholm. 2000
26. Muir-Wood, R. and King G. C. P. "Hydrological Signatures of Earthquake Strain." Journal of Geophysical Research, 98(B12), 22035-22068. 1993.
27. Wahlström, R. and Grünthal, G. "Probabilistic seismic hazard assessment (horizontal PGA) for Sweden, Finland and Denmark using the logic tree approach for regionalization and nonregionalization models." Seismological Research Letters, 2(1), 33-45. 2000.
28. Vermilye, J.M. and Scholz, C.H. "The process zone. A microstructural view of fault growth", J. Geophys. Res., 103(B6), 12223-12237.1998.